2010 IEEE International Conference on Robotics and Automation
Anchorage Convention District
May 3-8, 2010, Anchorage, Alaska, USA

Spring Assisted Modular and Reconfigurable Robot: Design, Analysis and Control

Guangjun Liu, *Senior Member, IEEE* and Yugang Liu

Abstract— **This paper presents an innovative spring assisted modular and reconfigurable robot (MRR) design and control framework, which is developed based on a synergetic integration of robot control with a brake and an embedded spring at each modular joint. By activating the brake, static balancing can be established, allowing reinforced delicate operation in the neighborhood of a balanced configuration such as door opening, as well as spring assisted lift of heavy payload. The developed spring assisted MRR can improve the payload to weight ratio of the conventional robot manipulators without introducing sophisticated mechanisms. A distributed control method has been proposed to facilitate control of the spring assisted MRR. The developed control algorithm does not rely on a prior dynamic models and can suppress uncertainties introduced by module reconfigurations as well as uncertainties due to sensor inaccuracies and noises. With the developed controller, control parameters need not to be adjusted when adding modules to or removing modules from an MRR, or changing its configurations. Prototype modules have been developed, and the experimental results have confirmed the effectiveness of the proposed design and control.**

I. INTRODUCTION

With substantial application potential especially in aerospace sector, the development of modular and reconfigurable robots (MRRs) is one of the most promising research areas in robotics [1]. However, the payload and manipulation capability of conventional modular manipulators is severely limited compared to their own weight, and a large portion of the actuator output is used to compensate the weight of the robot joints and links. Such problems become more severe when they are expanded by adding pre-designed modules, and the development of MRRs with improved payload to weight ratio is essential.

In related research works on MRRs, three types of MRRs have been reported in terms of self-reassembly, self-reconfigurable and manually-reconfigurable modular robots. The modular robotic concept can be traced back to 1980's and a generalized modular architecture for robot structures was presented in [2]. The main concept of developing reconfigurable robots is based on the use of modular components as building blocks, which may result in various mechanical modules. Conventional robot control methods are based on known robot configuration and its associated dynamic model, and automatic model generation for MRRs used to be a hot research topic [3]. However, the control parameters have to be retuned according to the regenerated models due to the unmodeled system dynamics caused by reconfiguration [4]. Recently in our laboratory, a distributed MRR control system has been developed based on joint torque sensing [5].

Extensive efforts have been reported to improve the payload capability of robotic manipulators. The robot weight is substantially reduced by taking advantage of technology advancement such as development of actuator and link using advanced materials [6]. This approach is effective but requires expensive hardware development and fabrication. In the literature, static balancing with counterweights and external springs has been used to compensate for robot body weight, but it involves sophisticated mechanisms and restricts the working envelope of the robot [7]–[9]. In [10], a spring is used to counter-balance gravitational torque applied to an MRR module, and a loading plate with a loading pin is used to manually set the preloaded torque of the module.

This paper presents the design and control of a proposed spring assisted MRR that has a spring and an associated brake embedded in each joint module. The power spring and a decoupling bearing are inserted between the brake and the actuator shaft. By activating the brake, static balancing can be established. The MRR manipulation capability and payload capacity are henceforth boosted with a synergetic integration of our proposed multiple mode MRR control with the introduced joint brake and spring. Energy can be accumulated in the spring and released in a controlled manner to reinforce the robot manipulation capability. With the assistance of the power spring, the actuators can be kept away from saturation to maintain proper operation of the control law when heavy payloads are handled.

Joint brakes are conventionally required to lock the robot while power is off. The proposed design boosts the actuator torque output by taking advantage of the existing brake and requires minimum additional hardware and associated weight. In this paper, a distributed control method is developed based on torque sensing to control the proposed joint module with the spring activated or deactivated, which can be used to control MRRs with any number of modules and with any robotic configurations. Two prototype modules with embedded power spring are developed in our laboratory to validate the design concepts, and experimental results have verified the effectiveness of the proposed design and control.

The rest of the paper is organized as follows: Section II presents the mechanical design of the joint with brake and spring. Section III presents modeling and motion control design. Experimental results are presented in Section IV. Concluding remarks and discussions are given in Section V.

Manuscript received September 15, 2009. This work was supported in part by a grant from Natural Sciences and Engineering Research Council (NSERC), Canada, and in part by Engineering Services Inc.

The authors are with Department of Aerospace Engineering, Ryerson University, 350 Victoria St., Toronto, Ontario Canada M5B 2K3. (Email: gjliu@ryerson.ca, ygliu@ryerson.ca

II. MRR Module with Embedded Spring

Several MRR modules are developed in our laboratory recently. Each module consists of components such as actuator, encoder, speed reducer, joint torque sensor and a brake. Besides these common components, the newly developed module with an embedded power spring is as shown in Fig. 1. As illustrated in Fig. 1), the power spring is inserted between the brake rotor and the actuator shaft through a decoupling bearing. One side of the spring is connected with the actuator shaft, and the other side to the rotor of the brake. If the brake is in the released state, the spring and brake rotor rotate together with the actuator shaft. When the brake is activated, the brake rotor is brought to a halt, but the actuator shaft can still rotate. As a result, the spring generates a moment that grows with the shaft position change from the position when the brake was activated (locking position). The spring generated moment (SGM) can then be used to assist the actuator in robot operations.

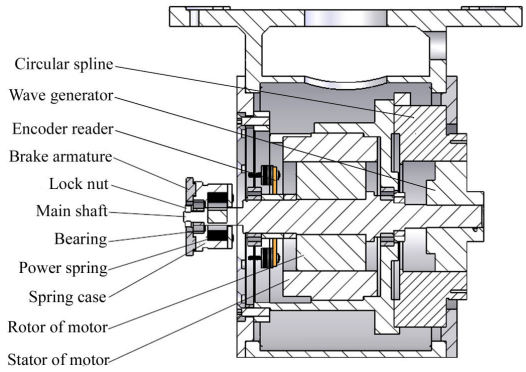

(a)

Fig. 1. Mechanism design for a spring-assisted modular joint.

The torque vs. deflection relationship for a power spring can be approximated by [11]:

$$\frac{\tau_k}{T_{kmax}} \approx 1 - \left(\frac{u}{U_{max}} - 1\right)^2 \tag{1}$$

where τ_k is the SGM; u denotes the deformation of the spring; similarly, T_{kmax} and U_{max} represent the maximum SGM and the maximum deformation of the spring.

The brake can be activated at any joint position by the controller to set the locking position q_l. Thereafter at any joint position q, the SGM can be calculated as

$$\tau_k = T_{kmax}\left\{1 - \left[\frac{\gamma\,(q_l - q)}{U_{max}} - 1\right]^2\right\} \tag{2}$$

where γ is the reduction ratio of the speed reducer. q_l and q are defined as the link side positions.

III. Control Design and Application of Module with Embedded Spring

A. Dynamic Model Formulation

Consider MRRs with the proposed modules installed in series as illustrated in Fig. 2. Each module provides a rotary joint. Modules close to the base module are named

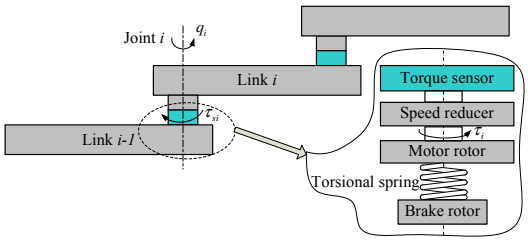

Fig. 2. Schematic diagram of a proposed MRR

lower modules, and modules close to the end-effector are called upper modules. To derive the dynamic equations, the following assumptions are made: the rotor is assumed to be symmetric with respect to the rotation axis; flexibility of the joint shaft and the speed reducer is assumed to be negligible, which is reasonable for harmonic drive, a kind of "zero" backlash gearhead; it is assumed that the torque transmission does not fail at the speed reducer, and the inertia between the torque sensor and the speed reducer is negligible; inertial moment of the spring and brake rotor is assumed to be negligible compared with that of the actuator rotor and shaft.

Based on the dynamic equations of a rigid robot manipulator with n rotary joints and joint torque sensing [5], the dynamic equations for MRRs with embedded spring can be formulated as follows:

For the base module, $i = 1$

$$I_{m1}\gamma_1\ddot{q}_1 - \tau_{k1} + f_1(q_1, \dot{q}_1) + \frac{\tau_{s1}}{\gamma_1} = \tau_1 \tag{3}$$

For the second module from the base, $i = 2$

$$I_{m2}\gamma_2\ddot{q}_2 - \tau_{k2} + f_2(q_2, \dot{q}_2) + I_{m2}z_2^T z_1\ddot{q}_1 + \frac{\tau_{s2}}{\gamma_2} = \tau_2 \tag{4}$$

For the upper modules, $i \geq 3$

$$\begin{aligned} &I_{mi}\gamma_i\ddot{q}_i - \tau_{ki} + f_i(q_i, \dot{q}_i) + I_{mi}\sum_{j=1}^{i-1} z_i^T z_j\ddot{q}_j \\ &+\tfrac{\tau_{si}}{\gamma_i} + I_{mi}\sum_{j=2}^{i-1}\sum_{k=1}^{j-1} z_i^T(z_k \times z_j)\dot{q}_k\dot{q}_j = \tau_i \end{aligned} \tag{5}$$

In the derived dynamic equations (3)–(5), I_{mi} is the moment of inertia of the rotor about the axis of rotation; τ_{si} is the coupling torque with the upper modules at the torque sensor location; and τ_i is the actuator output torque; and the SGM for the i^{th} module τ_{ki} can be derived from (2) as follows:

$$\tau_{ki} = \begin{cases} k_{i1}\gamma_i\,(q_{li} - q_i) + k_{i2}\gamma_i^2\,(q_{li} - q_i)^2, & brake\ engaged \\ 0, & brake\ released \end{cases} \tag{6}$$

where $k_{i1} = \frac{2T_{kimax}}{U_{imax}}$ and $k_{i2} = -\frac{T_{kimax}}{U_{imax}^2}$.

The joint friction, $f_i(q_i, \dot{q}_i)$, is assumed to be a function of the joint position and velocity [12]:

$$\begin{aligned} f_i(q_i, \dot{q}_i) = &\left[f_{ci} + f_{si}\exp(-f_{\tau i}\dot{q}_i^2)\right] sgn(\dot{q}_i) \\ &+b_i\dot{q}_i + f_{qi}(q_i, \dot{q}_i) \end{aligned} \tag{7}$$

where f_{ci} denotes the Coulomb friction related parameter; f_{si} denotes the static friction related parameter; $f_{\tau\,i}$ is a

positive parameter corresponding to the Stribeck effect; b_i denotes the viscous friction coefficient; $f_{qi}(q_i, \dot{q}_i)$ reflects the position dependency of friction and other friction modeling errors; and $sgn(\dot{q}_i)$ is the sign function.

Let $F_i = [b_i \ f_{ci} \ f_{si} \ f_{\tau i}]^T$, $\Theta_{ijk} = z_i^T (z_k \times z_j)$ and $\theta_{ij} = z_i^T z_j$, according to the model uncertainty decomposition scheme proposed by Liu, [13], θ_{ij}, Θ_{ijk} and F_i can be decomposed into a constant part plus a variable part, i.e.,

$$\begin{aligned} \theta_{ij} &= \theta_{ij}^c + \theta_{ij}^v \\ \Theta_{ijk} &= \Theta_{ijk}^c + \Theta_{ijk}^v \\ F_i &= F_i^c + F_i^v \end{aligned} \tag{8}$$

where the superscripts 'c' and 'v' denote the constant and variable parts, respectively.

Let $\hat{b}_i^c$, $\hat{f}_{ci}^c$, $\hat{f}_{si}^c$ and $\hat{f}_{\tau i}^c$ represent estimates of constant friction parameters, using the linearization scheme proposed by Liu in [14], the friction model shown in (7) can be approximated by:

$$f_i(q_i, \dot{q}_i) \approx \hat{f}_i^c(\dot{q}_i) + Y(\dot{q}_i)\left(\tilde{F}_i^c + F_i^v\right) + f_{qi}(q_i, \dot{q}_i) + \check{f}_i(\dot{q}_i) \tag{9}$$

where $\tilde{F}_i^c = F_i^c - \hat{F}_i^c$ with $\hat{F}_i^c = [\hat{b}_i^c \ \hat{f}_{ci}^c \ \hat{f}_{si}^c \ \hat{f}_{\tau i}^c]^T$; $\hat{f}_i^c(\dot{q}_i)$, $\check{f}_i(\dot{q}_i)$ and $Y(\dot{q}_i)$ can be detailed as follows:

$$\begin{aligned} \hat{f}_i^c(\dot{q}_i) &= \left[\hat{f}_{ci}^c + \hat{f}_{si}^c \exp\left(-\hat{f}_{\tau i}^c \dot{q}_i^2\right)\right] sat(\dot{q}_i, \epsilon_{\dot{q}_i}) + \hat{b}_i^c \dot{q}_i \\ \check{f}_i(\dot{q}_i) &= \left[f_{ci} + f_{si} \exp\left(-f_{\tau i} \dot{q}_i^2\right)\right] [sgn(\dot{q}_i) - sat(\dot{q}_i, \epsilon_{\dot{q}_i})] \\ Y(\dot{q}_i) &= \left[0 \ \ 1 \ \ \exp(-\hat{f}_{\tau i}^c \dot{q}_i^2) \ \ -\hat{f}_{si}^c \dot{q}_i^2 \exp(-\hat{f}_{\tau i}^c \dot{q}_i^2)\right] \\ &\quad \cdot sat(\dot{q}_i, \epsilon_{\dot{q}_i}) + \left[\dot{q}_i \ \ 0 \ \ 0 \ \ 0\right] \end{aligned} \tag{10}$$

where the saturation function is defined as follows:

$$sat(\dot{q}_i, \epsilon_{\dot{q}_i}) = \begin{cases} \frac{\dot{q}_i}{|\dot{q}_i|}, & |\dot{q}_i| > \epsilon_{\dot{q}_i} \\ \frac{\dot{q}_i}{\epsilon_{\dot{q}_i}}, & |\dot{q}_i| \le \epsilon_{\dot{q}_i} \end{cases} \tag{11}$$

where $\epsilon_{\dot{q}_i}$ is a positive constant.

Property 1:

$$|\theta_{ij}^v| < \rho_{\theta ij}, |\Theta_{ijk}^v| < \rho_{\Theta ijk}, |F_{ij}^v| < \rho_{Fij} (j = 1 \cdots 4) \tag{12}$$

where $\rho_{\theta ij}$, $\rho_{\Theta_{ijk}}$ and $\rho_{F_i j}$ are known constant bounds.

Property 2:

$$|f_{qi}(q_i, \dot{q}_i)| < \rho_{fqi} \tag{13}$$

where ρ_{fqi} is a known constant bound for any position q_i and velocity $\dot{q}_i$.

Property 3:

$$|\tau_{si} - \hat{\tau}_{si}| < \rho_{\tau si} \tag{14}$$

where $\hat{\tau}_{si}$ denotes the measured coupling torque at the torque sensor location, and $\rho_{\tau si}$ is a known constant bound.

Property 4:

$$|\ddot{e}_i| \le \rho_{eai}, \quad |\dot{e}_i| \le \rho_{evi} \tag{15}$$

where ρ_{eai} and ρ_{evi} are known constant bounds.

Property 5:

$$|\theta_{ij}| = |z_i^T z_j| \le 1, \quad |\Theta_{ijk}| = |z_i^T (z_k \times z_j)| \le 1 \tag{16}$$

Property 6:

$$|\check{f}_i(\dot{q}_i)| < \rho_{fi} \tag{17}$$

B. Control Design

According to the torque sensing based distributed MRR control algorithm developed in [5], the control input τ_i can be designed joint by joint; and the model uncertainties are all bounded. The system errors are defined as:

$$\begin{aligned} e_i &:= q_i - q_{id} \\ r_i &:= \dot{e}_i + \lambda_i e_i \\ a_i &:= \ddot{q}_{id} - 2\lambda_i \dot{e}_i - \lambda_i^2 e_i \end{aligned} \tag{18}$$

where q_{id} and $\ddot{q}_{id}$ represent the desired joint positions and joint accelerations, respectively; and λ_i is a positive constant.

To stabilize the base joint, the control is designed as:

$$\begin{aligned} \tau_1 = I_{m1}\gamma_1 a_1 + \tfrac{\hat{\tau}_{s1}}{\gamma_1} - \hat{\tau}_{k1} \\ + \hat{f}_1^c(\dot{q}_1) - k_{I1} \textstyle\int_0^t r_1(t)\, dt + \tau_{r1} \end{aligned} \tag{19}$$

where $k_{I1} > 0$ is a constant and τ_{r1} is the decomposition-based robust control term [13], which is defined as:

$$\begin{aligned} \tau_{r1} = &-\left(\rho_{f1} + \rho_{fq1} + \tfrac{\rho_{\tau s1}}{\gamma_1}\right) \cdot sat(r_1, \epsilon_{r1}) \\ &- \sum_{j=1}^{4} \left\{ \rho_{F1j} Y_j(\dot{q}_1)\ sat\left(r_1 Y_j(\dot{q}_1), \epsilon_{F1j}\right) \right\} \end{aligned} \tag{20}$$

where $Y_j(\dot{q}_1)$ is the j^{th} element of $Y(\dot{q}_1)$; ϵ_{r1} and ϵ_{F1j} are positive control parameters.

The stabilization of the first joint results in boundedness of the magnitudes of $\dot{q}_1$ and $\ddot{q}_1$. Then, the control torque for the second joint, $i = 2$ can be designed as follows:

$$\begin{aligned} \tau_2 = I_{m2}\gamma_2 a_2 + \tfrac{\hat{\tau}_{s2}}{\gamma_2} - \hat{\tau}_{k2} - k_{I2} \textstyle\int_0^t r_2(t)\, dt \\ + \hat{f}_2^c(\dot{q}_2) + I_{m2}\hat{\theta}_{21}^c \ddot{q}_{1d} + \tau_{r2} \end{aligned} \tag{21}$$

where $k_{I2} > 0$ and τ_{r2} is defined as follows

$$\begin{aligned} \tau_{r2} = &-\left(\rho_{f2} + \rho_{fq2} + \tfrac{\rho_{\tau s2}}{\gamma_2} + I_{m1}\rho_{ea1}\right) sat(r_2, \epsilon_{r2}) \\ &- \sum_{j=1}^{4} \left\{ \rho_{F2j} Y_j(\dot{q}_2)\ sat\left(r_2 Y_j(\dot{q}_2), \epsilon_{F2j}\right) \right\} \\ &- I_{m1}\rho_{\theta 21} \ddot{q}_{1d} \cdot sat\left(r_2 \ddot{q}_{1d}, \epsilon_{\theta 21}\right) \end{aligned} \tag{22}$$

where ϵ_{r2}, $\epsilon_{\theta 21}$ and ϵ_{F2j} are positive control parameters.

Similarly, the control torque for the i^{th} joint can be designed as follows:

$$\begin{aligned} \tau_i = I_{mi}\gamma_i a_i + \tfrac{\hat{\tau}_{si}}{\gamma_i} - \hat{\tau}_{ki} - k_{Ii} \textstyle\int_0^t r_i(t)\, dt + \hat{f}_i^c(\dot{q}_i) \\ + I_{mi}\Big\{ \sum_{j=1}^{i-1} \hat{\theta}_{ij}^c \ddot{q}_{jd} + \sum_{j=2}^{i-1} \sum_{k=1}^{j-1} \hat{\Theta}_{ijk}^c \dot{q}_k \dot{q}_j \Big\} + \tau_{ri} \end{aligned} \tag{23}$$

where $k_{Ii} > 0$; and τ_{ri} is designed as follows:

$$\begin{aligned} \tau_{ri} = &-\left(\rho_{fi} + \rho_{fqi} + \tfrac{\rho_{\tau si}}{\gamma_i} + I_{mi} \sum_{j=1}^{i-1} \rho_{eaj}\right) sat(r_i, \epsilon_{ri}) \\ &- \sum_{j=1}^{4} \left\{ \rho_{Fij} Y_j(\dot{q}_i)\ sat\left(r_i Y_j(\dot{q}_i), \epsilon_{Fij}\right) \right\} \\ &- I_{mi} \sum_{j=1}^{i-1} \left\{ \rho_{\theta ij}\, \ddot{q}_{jd}\, sat\left(r_i \ddot{q}_{jd}, \epsilon_{\theta ij}\right) \right\} \\ &- I_{mi} \sum_{j=2}^{i-1} \sum_{k=1}^{j-1} \left\{ \rho_{\Theta ijk} \dot{q}_k \dot{q}_j\, sat\left(r_i \dot{q}_k \dot{q}_j, \epsilon_{\Theta ijk}\right) \right\} \end{aligned} \tag{24}$$

where ϵ_{ri}, ϵ_{Fij}, $\epsilon_{\theta ij}$, $\epsilon_{\Theta ijk}$ are positive control parameters; the estimated SGM $\hat{\tau}_{ki}$ can be achieved by replacing k_{i1}, k_{i2} with their estimates $\hat{k}_{i1}$, $\hat{k}_{i2}$ in (6).

The adaption law is given as follows:

$$\begin{aligned}
\dot{\hat{k}}_{i1} &= \begin{cases} \mu_{ki1}\gamma_i \left(q_{li}-q_i\right) r_i, & brake\ engaged \\ 0, & brake\ released \end{cases} \\
\dot{\hat{k}}_{i2} &= \begin{cases} \mu_{ki2}\gamma_i^2 \left(q_{li}-q_i\right)^2 r_i, & brake\ engaged \\ 0, & brake\ released \end{cases} \\
\dot{\hat{F}}_i^c &= -\mu_{Fic}\left[Y\left(\dot{q}_i\right)\right]^T r_i \\
\dot{\hat{\theta}}_{ij}^c &= -\mu_{\theta ij}\ddot{q}_{jd} r_i \\
\dot{\hat{\Theta}}_{ijk}^c &= -\mu_{\Theta ijk}\dot{q}_k\dot{q}_j r_i
\end{aligned} \tag{25}$$

where μ_{ki1}, μ_{ki2}, μ_{Fic}, $\mu_{\theta ij}$ and $\mu_{\Theta ijk}$ are positive constants.

Theorem: Given an n-DOF modular robot, with the joint dynamics as given in (3)–(5), and model uncertainty defined by (8), the tracking error of each joint is uniformly ultimately bounded under the control law given by (23) and the adaption law shown in (25).

Proof: Consider the Lyapunov function candidate

$$\begin{aligned}
V = &\tfrac{1}{2}I_{mi}\gamma_i r_i^2 + \tfrac{1}{2}k_{Ii}\left[\int_0^t r_i\left(t\right)dt\right]^2 + \tfrac{1}{2}\tfrac{\left(\tilde{F}_i^c\right)^T\tilde{F}_i^c}{\mu_{Fic}} + \tfrac{1}{2}\tfrac{\tilde{k}_{i1}^2}{\mu_{ki1}} \\
&+\tfrac{1}{2}\tfrac{\tilde{k}_{i2}^2}{\mu_{ki2}} + \tfrac{I_{mi}}{2}\sum_{j=1}^{i-1}\tfrac{\left(\tilde{\theta}_{ij}^c\right)^2}{\mu_{\theta ij}} + \tfrac{I_{mi}}{2}\sum_{j=2}^{i-1}\sum_{k=1}^{j-1}\tfrac{\left(\tilde{\Theta}_{ijk}^c\right)^2}{\mu_{\Theta ijk}}
\end{aligned} \tag{26}$$

Differentiating (26) yields

$$\begin{aligned}
\dot{V} = &r_i\left\{I_{mi}\gamma_i\dot{r}_i + k_{Ii}\int_0^t r_i\left(t\right)dt\right\} + \tfrac{\left(\dot{\tilde{F}}_i^c\right)^T\tilde{F}_i^c}{\mu_{Fic}} + \tfrac{\tilde{k}_{i1}\dot{\tilde{k}}_{i1}}{\mu_{ki1}} \\
&+\tfrac{\tilde{k}_{i2}\dot{\tilde{k}}_{i2}}{\mu_{ki2}} + I_{mi}\sum_{j=1}^{i-1}\tfrac{\tilde{\theta}_{ij}^c\dot{\tilde{\theta}}_{ij}^c}{\mu_{\theta ij}} + I_{mi}\sum_{j=2}^{i-1}\sum_{k=1}^{j-1}\tfrac{\tilde{\Theta}_{ijk}^c\dot{\tilde{\Theta}}_{ijk}^c}{\mu_{\Theta ijk}}
\end{aligned} \tag{27}$$

For the i^{th} joint, from *Properties 2–6*, if $|r_i| > \epsilon_{ri}$,

$$\begin{aligned}
&r_i\left\{\rho_{eaj}\ sat\left(r_i,\epsilon_{ri}\right) + \theta_{ij}\ddot{e}_j\right\} > 0 \\
&r_i\left\{\rho_{fqi}\ sat\left(r_i,\epsilon_{ri}\right) + f_{qi}\left(q_i,\dot{q}_i\right)\right\} > 0 \\
&r_i\left\{\rho_{fi}\ sat\left(r_i,\epsilon_{ri}\right) + \check{f}_i\left(\dot{q}_i\right)\right\} > 0 \\
&r_i\left\{\rho_{\tau si}\, sat\left(r_i,\epsilon_{ri}\right) + \tilde{\tau}_{si}\right\} > 0
\end{aligned} \tag{28}$$

If $|r_i| \le \epsilon_{ri}$,

$$\begin{aligned}
&r_i\left\{\rho_{eaj} sat\left(r_i,\epsilon_{ri}\right) + \theta_{ij}\ddot{e}_j\right\} \ge \rho_{eaj} r_i\left\{\tfrac{r_i}{\epsilon_{ri}} - \tfrac{r_i}{|r_i|}\right\} \\
&r_i\left\{\rho_{fqi}\ sat\left(r_i,\epsilon_{ri}\right) + f_{qi}\left(q_i,\dot{q}_i\right)\right\} \ge \rho_{fqi} r_i\left\{\tfrac{r_i}{\epsilon_{ri}} - \tfrac{r_i}{|r_i|}\right\} \\
&r_i\left\{\rho_{fi}\ sat\left(r_i,\epsilon_{ri}\right) + \check{f}_i\left(\dot{q}_i\right)\right\} \ge \rho_{fi} r_i\left\{\tfrac{r_i}{\epsilon_{ri}} - \tfrac{r_i}{|r_i|}\right\} \\
&r_i\left\{\rho_{\tau si} sat\left(r_i,\epsilon_{ri}\right) + \tilde{\tau}_{si}\right\} \ge \rho_{\tau si} r_i\left\{\tfrac{r_i}{\epsilon_{ri}} - \tfrac{r_i}{|r_i|}\right\}
\end{aligned} \tag{29}$$

For the i^{th} joint, with $j = 1, \cdots, 4$, if $|r_i Y_j\left(\dot{q}_i\right)| > \epsilon_{Fij}$, from *Property 1* and (11), we can obtain

$$r_i Y_j\left(\dot{q}_i\right)\left\{\rho_{Fij} sat\left(r_i Y_j\left(\dot{q}_i\right),\epsilon_{Fij}\right) + F_{ij}^v\right\} > 0 \tag{30}$$

If $|r_i Y_j\left(\dot{q}_i\right)| \le \epsilon_{Fij}$,

$$\begin{aligned}
&r_i Y_j\left(\dot{q}_i\right)\left\{\rho_{Fij} sat\left(r_i Y_j\left(\dot{q}_i\right),\epsilon_{Fij}\right) + F_{ij}^v\right\} \\
&\quad \ge \rho_{Fij} r_i Y_j\left(\dot{q}_i\right)\left\{\tfrac{r_i Y_j(\dot{q}_i)}{\epsilon_{Fij}} - \tfrac{r_i Y_j(\dot{q}_i)}{|r_i Y_j(\dot{q}_i)|}\right\}
\end{aligned} \tag{31}$$

For the i^{th} joint, with $j = 1, \cdots, i-1$, if $|r_i\ddot{q}_{jd}| > \epsilon_{\theta ij}$,

$$r_i\ddot{q}_{jd}\left\{\rho_{\theta ij} sat\left(r_i\ddot{q}_{jd},\epsilon_{\theta ij}\right) + \theta_{ij}^v\right\} > 0 \tag{32}$$

If $|r_i\ddot{q}_{jd}| \le \epsilon_{\theta ij}$,

$$\begin{aligned}
&r_i\ddot{q}_{jd}\left\{\rho_{\theta ij} sat\left(r_i\ddot{q}_{jd},\epsilon_{\theta ij}\right) + \theta_{ij}^v\right\} \\
&\quad \ge \rho_{\theta ij} r_i\ddot{q}_{jd}\left\{\tfrac{r_i\ddot{q}_{jd}}{\epsilon_{\theta ij}} - \tfrac{r_i\ddot{q}_{jd}}{|r_i\ddot{q}_{jd}|}\right\}
\end{aligned} \tag{33}$$

For the i^{th} joint, with $j = 2, \cdots, i-1$ and $k = 1, \cdots, j-1$, if $|r_i\dot{q}_k\dot{q}_j| > \epsilon_{\Theta ijk}$,

$$r_i\dot{q}_k\dot{q}_j\left\{\rho_{\Theta ijk} sat\left(r_i\dot{q}_k\dot{q}_j,\epsilon_{\Theta ijk}\right) + \Theta_{ijk}^v\right\} > 0 \tag{34}$$

If $|r_i\dot{q}_k\dot{q}_j| \le \epsilon_{\Theta ijk}$,

$$\begin{aligned}
&r_i\dot{q}_k\dot{q}_j\left\{\rho_{\Theta ijk} sat\left(r_i\dot{q}_k\dot{q}_j,\epsilon_{\Theta ijk}\right) + \Theta_{ijk}^v\right\} \\
&\quad \ge \rho_{\Theta ijk} r_i\dot{q}_k\dot{q}_j\left\{\tfrac{r_i\dot{q}_k\dot{q}_j}{\epsilon_{\Theta ijk}} - \tfrac{r_i\dot{q}_k\dot{q}_j}{|r_i\dot{q}_k\dot{q}_j|}\right\}
\end{aligned} \tag{35}$$

The right-side terms of (29), (31), (33) and (35) achieve the minimum values at $|r_i| = \frac{\epsilon_{ri}}{2}$, $|r_i Y_j\left(\dot{q}_i\right)| = \frac{\epsilon_{Fij}}{2}$, $|r_i\ddot{q}_{jd}| = \frac{\epsilon_{\theta ij}}{2}$ and $|r_i\dot{q}_k\dot{q}_j| = \frac{\epsilon_{\Theta ijk}}{2}$, respectively. With consideration that $\dot{\tilde{k}}_{i1} = -\dot{\hat{k}}_{i1}$, $\dot{\tilde{k}}_{i2} = -\dot{\hat{k}}_{i2}$, $\dot{\tilde{F}}_i^c = -\dot{\hat{F}}_i^c$, $\dot{\tilde{\theta}}_{ij}^c = -\dot{\hat{\theta}}_{ij}^c$ and $\dot{\tilde{\Theta}}_{ijk}^c = -\dot{\hat{\Theta}}_{ijk}^c$, we have

$$\begin{aligned}
\dot{V} \le &-I_{mi}\gamma_i\lambda_i r_i^2 + I_{mi}\left\{\sum_{j=1}^{i-1}\tfrac{\rho_{\theta ij}\epsilon_{\theta ij}}{4} + \sum_{j=2}^{i-1}\sum_{k=1}^{j-1}\tfrac{\rho_{\Theta ijk}\epsilon_{\Theta ijk}}{4}\right\} \\
&+\sum_{j=1}^{4}\left\{\tfrac{\rho_{Fij}\epsilon_{Fij}}{4}\right\} + \tfrac{\epsilon_{ri}}{4}\left\{I_{mi}\sum_{j=1}^{i-1}\rho_{eaj} + \rho_{fqi} + \rho_{fi} + \tfrac{\rho_{\tau si}}{\gamma_i}\right\}
\end{aligned} \tag{36}$$

From (36), V is a Lyapunov function only when

$$|r_i| > \sqrt{\frac{\begin{aligned}&I_{mi}\sum_{j=1}^{i-1}\left\{\tfrac{\rho_{\theta ij}\epsilon_{\theta ij}+\rho_{eaj}\epsilon_{ri}}{4}\right\} + \tfrac{\epsilon_{ri}\left\{\rho_{fqi}+\rho_{fi}+\frac{\rho_{\tau si}}{\gamma_i}\right\}}{4} \\ &+I_{mi}\sum_{j=2}^{i-1}\sum_{k=1}^{j-1}\left\{\tfrac{\rho_{\Theta ijk}\epsilon_{\Theta ijk}}{4}\right\} + \sum_{j=1}^{4}\left\{\tfrac{\rho_{Fij}\epsilon_{Fij}}{4}\right\}\end{aligned}}{I_{mi}\gamma_i\lambda_i}} \tag{37}$$

Let Γ represents the right-side term of (37), and define $S = \left\{r_i \in \Re | r_i^2 \le 2\Gamma^2\right\}$. On the surface of S, ∂S, we have

$$\dot{V} \le -I_{mi}\gamma_i\lambda_i\Gamma^2 \tag{38}$$

Denote t_s as the time for the solution trajectory to intersect the surface ∂S, then

$$\frac{V\left(r_i\left(t_s\right)\right) - V\left(r_i\left(0\right)\right)}{t_s} \le -I_{mi}\gamma_i\lambda_i\Gamma^2 \tag{39}$$

Furthermore,

$$t_s \le \frac{V\left(r_i\left(0\right)\right) - V\left(r_i\left(t_s\right)\right)}{I_{mi}\gamma_i\lambda_i\Gamma^2} \tag{40}$$

Therefore, r_i is bounded, which indicates that e_i and $\dot{e}_i$ are bounded as per the proof developed by Slotine and Li [15]. Furthermore, as $\epsilon_{ri}, \epsilon_{Fij}, \epsilon_{\theta ij}, \epsilon_{\Theta ijk} \to 0$, $S \to \mathbf{0}$, which means $|r_i| \to 0$, as followed by $e_i, \dot{e}_i \to 0$. ■

IV. Experiments

A. Experimental Setup

The experimental setup consists of two MRR modules developed in our laboratory, as shown in Fig. 3(b). The upper module contains embedded power spring, as shown in Fig. 1. The design parameters for the MRR modules, the control parameters, as well as the parametric uncertainty bounds adopted in the experiments are listed in Tab. I. Experiments are conducted with one MRR module and two MRR modules, respectively.

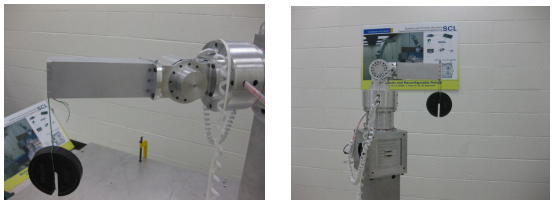

(a) (b)

Fig. 3. Experimental setup: (a) spring assisted motion; (b) tracking control.

TABLE I

Design parameters and control parameters

Design and control parameters				Uncertainty bounds	
I_{m1}	0.2472	ϵ_{Fi1}	10^{-4}	ρ_{Fi1}	10^{-3} (Nms/rad)
I_{m2}	0.0346	ϵ_{Fi2}	10^{-3}	ρ_{Fi2}	10^{-2} (Nm)
k_{Ii}	10.0	ϵ_{Fi3}	10^{-3}	ρ_{Fi3}	10^{-2} (Nm)
γ_i	101	ϵ_{Fi4}	0.10	ρ_{Fi4}	1.0 (s^2/rad^2)
λ_i	160	$\epsilon_{\dot{q}_i}$	0.01	ρ_{fqi}	0.5 (N m)
$\mu_{\theta ij}$	0.01	$\epsilon_{\theta ij}$	0.10	$\rho_{\theta ij}$	1.0
$\mu_{\Theta ijk}$	0.01	$\epsilon_{\Theta ijk}$	0.10	$\rho_{\Theta ijk}$	1.0
μ_{ki}	1.00	ϵ_{ri}	0.10	$\rho_{\tau si}$	1.0 (N m)
μ_{Fic}	0.10			ρ_{eai}	0.01 (rad/s^2)

$(\star)$: the unit of inertial moment is $g\,m^2$.

B. Experimental Results

1) Spring Assisted Motion: To investigate how the spring can assist the actuator to achieve better performance with less power consumption, experiments are conducted with one MRR module (Joint 2), so as to keep such influential factors as coupling and interactions between different joints out of the loop, as shown in Fig. 3(a). The equilibrium position for Joint 2 is set at $q_{e2} = 0^\circ$ (as seen from the link side), where the gravity generated moment reaches its maximum. Joint 2 is controlled to track a cosinusoidal position trajectory started from the equilibrium position $q_{e2} = 0^\circ$ for two different cases: one is with the brake engaged and the other is with the brake released. In these experiments, a $10 - N$ weight is attached to the end of the link through a cable, and the distance between the attaching point and the axis of Joint 2 is $0.30\ m$, as shown in Fig. 3(a).

Fig. 4(a) shows the desired and the controlled trajectories with and without brake activation, respectively. The tracking position errors and the corresponding control inputs for the tests with and without activating the spring are compared in Figs. 4(b)–(c). To confirm the effectiveness of the proposed

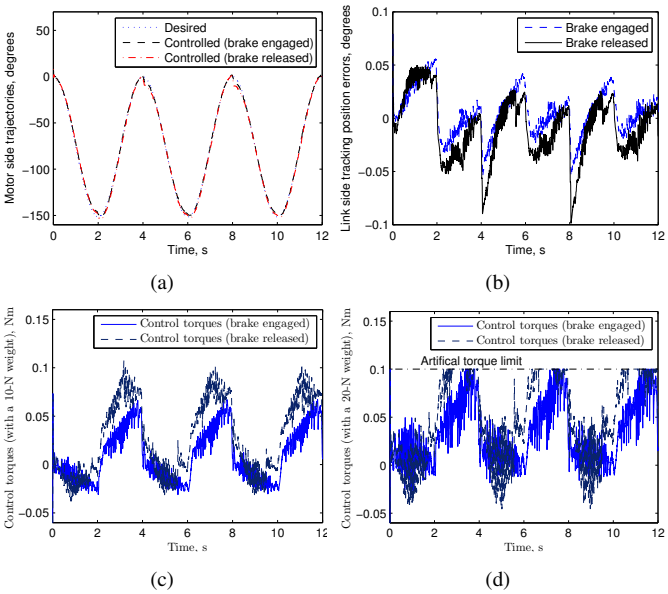

Fig. 4. Experimental results for spring-assisted motion.

TABLE II

Experimental results for spring assisted motion

Brake	$\max\{\lvert e_2(i)\rvert\}$	$\sqrt{\frac{\sum_{i=1}^{N} e_2^2(i)}{N}}$	$\max\{\lvert\tau_2(i)\rvert\}$	$\sqrt{\frac{\sum_{i=1}^{N} \tau_2^2(i)}{N}}$
Engaged	0.079°	0.023°	$0.09\ Nm$	$0.03\ Nm$
Released	0.099°	0.031°	$0.11\ Nm$	$0.05\ Nm$

spring assisted robot control approach, a comparison of the control performance and the control inputs is made between the cases with and without activating the spring, and the results are shown in Tab. II. In Tab. II, $N = 6000$ is the total number of sampling points, $e_2(i)$ and $\tau_2(i)$ represent the tracking error and control torques for the second joint at the time instant of the i^{th} sampling point, as seen from the motor side. When the brake is activated, with the assistance of the spring, the actuator torque is 40% smaller, yet the tracking error is 25.81% smaller while all the control parameters are kept the same. Furthermore, the maximum position error and the required peak control torque have also been reduced, as shown in Tab. II.

2) Handling Heavy Payload: To study how the spring can help the actuator lift a heavy payload without actually reaching the physical limits of the joint modules, the actuator maximum output torque of Joint 2 is artificially limited to 20% of its ratings, i.e., $\tau_{max} = 0.1\ Nm$. A $20 - N$ weight is carried to follow the aforementioned cosinusoidal trajectory.

The actuator torques are compared for the tests with and without the spring assistance in Fig. 4(d). The robot failed to follow the desired trajectory without spring assistance because the motor was saturated. However, the case with brake activation finished the trajectory tracking task successfully.

Comparing the actuator torques required with and without spring assistance, one can see that the actuator torque is significantly reduced with the assistance of the spring. When the attached weight is increased to $50\ N$, the robot fails to lift the weight without the spring assistance.

3) Tracking Control: To verify the distributed control method developed in this paper, experiments are conducted with two MRR modules, as shown in Fig. 3(b). The brake of Joint 2 engaged and a $20 - N$ weight is attached. The equilibrium position for Joint 2 is selected to be $q_{e2} = 90°$, as seen from the link side. The same control parameters are selected for all the cases, as shown in Tab. I.

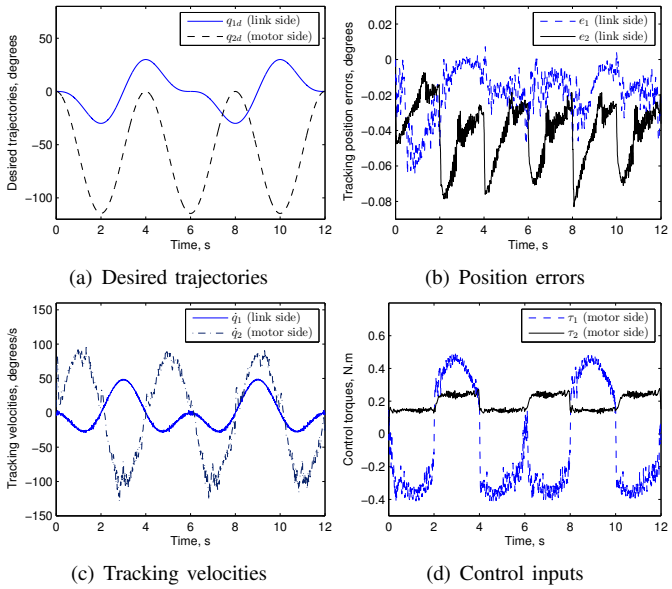

(a) Desired trajectories (b) Position errors

(c) Tracking velocities (d) Control inputs

Fig. 5. Experimental results for tracking control.

The experimental results for tracking control are shown in Fig. 5: the desired trajectories are shown in Fig. 5(a). Fig. 5(b) presents the corresponding tracking position errors. The tracking velocities are given by Fig. 5(c). And Fig. 5(d) shows the corresponding control inputs.

From the experimental results for spring-assisted motion and tracking control, we can see that the developed distributed algorithm can control MRRs to follow desired trajectories without adjusting the control parameters or deriving the dynamics models; and the control performance will not be affected by adding new modules or changing the configurations. And the uncertainties caused by reconfiguration can be suppressed effectively.

V. CONCLUSIONS AND DISCUSSIONS

This paper presents the design of a spring assisted MRR, which is equipped with a brake and an embedded spring at each module joint. This compact design does not introduce any sophisticated mechanism, and the overall working envelope will not be affected. A distributed control framework is developed to facilitate control of the spring assisted MRR. The spring can be activated or deactivated, so as to reinforce sophisticated manipulation in the neighborhood of a balanced configuration. With the assistance of the spring, the control performance can be improved with much less power consumption. The developed control method does not rely on a priori dynamic model and can suppress uncertainties due to reconfigurations and that caused by sensor inaccuracies and noises. With the developed control method, it is not necessary to adjust the control parameters when modules are added to or removed from an MRR, or when the configurations of the MRR are changed. The effectiveness of the proposed design and control are verified by some preliminary experiments on prototype modules developed in our laboratory.

In the proposed design, a power spring is inserted between the motor shaft and brake armature, so that the spring generated moment can be enlarged by the gear. However, this characteristic also limits the workspace of the joint upon spring activation, which is the maximum spring deformation divided by the gear ratio. Though the brake can be engaged at any configuration of the robot, it might still constrain some applications. To further verify the effectiveness of the proposed design, more MRR modules will be developed and further experiments will be conducted in our future research.

VI. ACKNOWLEDGMENTS

Useful discussions on spring assisted modular robots with Dr. Wen-Hong Zhu of the Canadian Space Agency, Canada, is gratefully acknowledged.

REFERENCES

[1] M. Yim, W.-M. Shen, B. Salemi, D. Rus, M. Moll, H. Lipson, E. Klavins, and G. S. Chirikjian, "Modular self-reconfigurable robot systems: challenges and opportunities for the future," *IEEE Robot. Autom. Mag.*, vol. 14, no. 1, pp. 43–52, Mar. 2007.

[2] D. Tesar and M. S. Butler, "A generalized modular architecture for robot structures," *ASME Trans. on Manufacturing Review*, vol. 2, no. 2, pp. 91–118, June 1989.

[3] I.-M. Chen, S. H. Yeo, G. Chen, and G. Yang, "Kernel for modular robot applications: automatic modeling techniques," *The Intl. J. of Robotics Research*, vol. 18, no. 2, pp. 225–242, Feb. 1999.

[4] W. W. Melek and A. A. Goldenberg, "Neurofuzzy control of modular and reconfigurable robots," *IEEE/ASME Trans. on Mechatronics*, vol. 8, no. 3, pp. 381–389, Sep. 2003.

[5] G. Liu, S. Abdul, and A. Goldenberg, "Distributed control of modular and reconfigurable robot with torque sensing," *Robotica*, vol. 26, no. 1, pp. 75–84, Jan. 2008.

[6] G. Hirzinger, N. Sporer, M. Schedl, J. Butterfaβ, and M. Grebenstein, "Torque-controlled lightweight arms and articulated hands: do we reach technological limits now?" *The Intl. J. of Robotics Research*, vol. 23, no. 4–5, pp. 331–340, April–May 2004.

[7] I. Simionescu and L. Ciupitu, "The static balancing of the industrial robot arms part i: discrete balancing," *Mechanism and Machine Theory*, vol. 35, pp. 1287–1298, 2000.

[8] A. Gopalswamy, P. Gupta, and M. Vidyasagar, "A new parallelogram linkage configuration for gravity compensation using torsional springs," in *Proc. IEEE Int. Conf. on Robotics and Automation*, Nice, France, May 1992, pp. 664–669.

[9] S. K. Agrawal and A. Fattah, "Reactionless robots: novel designs and concept studies," in *Proc. IEEE Int. Conf. on Control, Automation, Robotics and Vision*, Singapore, Dec. 2002, pp. 809–814.

[10] W.-H. Zhu, T. Lamarche, and P. Barnard, "Modular robot manipulators with preloadable modules," in *Proc. IEEE Int. Conf. on Mechatronics and Automation*, Harbin, China, Aug. 2007, pp. 7–12.

[11] J. E. Shigley and C. R. Mischke, *Standard handbook of machine desgin*, 2nd ed. Mcgraw-Hill Company, 1996.

[12] G. Liu, A. A. Goldenberg, and Y. Zhang, "Precise slow motion control of a direct-drive robot arm with velocity estimation and friction compensation," *Mechatronics*, vol. 14, no. 7, pp. 821–834, 2004.

[13] G. Liu and A. A. Goldenberg, "Uncertainty decomposition-based robust control of robot manipulators," *IEEE Trans. on Control Systems Technology*, vol. 4, no. 4, pp. 384–393, July 1996.

[14] G. Liu, "Decomposition-based friction compensation of mechanical systems," *Mechatronics*, vol. 12, no. 5, pp. 755–769, 2002.

[15] J. J. E. Slotine and W. Li, *Applied nonlinear control*. Englewood Cliffs, NJ: Prentice-Hall, 1991.